Plant-associated microbiome dynamics in a strip-cropped field

Enoch Narh Kudjordjie[1], Mette Vestergård[1], Mesfin T Gebremikael[2], Otto Nielsen[3], Mogens Nicolaisen[1]*

[1]Department of Agroecology, Faculty of Technical Sciences, Aarhus University, Slagelse 4200, Denmark.

[2]Department of Food Science - Plant, Food & Sustainability, Department of Food Science - Food Technology. Agro Food Park 48, 8200 Aarhus N, Denmark

[3]Nordic beet Research (NBR), Sofiehøj, Højbygårdvej 14, Denmark

*Correspondence: Mogens Nicolaisen (mn@agro.au.dk)

Abstract

Background

Diversified cropping systems including intercropping and strip cropping have generally been shown to be highly productive and resilient compared to monocropped systems. Enhanced agronomic and environmental benefits that characterize these systems minimize agrochemical use while maintaining high crop yields and production. While these benefits could be driven by higher microbial diversity sculpted by the distinct crop types, we still have limited insight into how plant microbiomes are assembled in these cropping systems at the field scale. Here, we examined the dynamics and site-specific assembly of soil and phyllosphere microbiomes in a rotational faba bean (FB) (*Vicia faba*) and spring barley (SB) (*Hordeum vulgare*) strip field during two cropping seasons. FB and SB were grown in neighbouring 6 m wide strips. Using bacterial 16S and fungal ITS amplicon sequencing, we analysed the microbial communities across gradients from the centre of strips towards the edge of strips, where FB and SB strips met.

Results

We found highly dynamic microbial communities that were distinct between the FB and SB strips and that varied across time. Within the strips, we observed a gradient-specific microbial distribution including some fungal pathogens. For instance, the genus *Puccinia* was

consistently enriched in the centre of the SB strips and gradually declined towards the edge of the strips. Neighbour strips affected the microbial richness in the adjacent strips with the strongest effects on the edge plants. Moreover, we observed distinct site-specific microbial interactions and bacterial and fungal co-occurrence networks within strip fields. Inter-phylum co-occurrence networks exhibited more dissimilar network configurations on the shoots than in the soil, primarily due to higher dynamic patterns of the phyllosphere microbiota in SB. Network tolerance to disturbance suggested that networks at the edge of the strips were more resilient to disturbances than networks in the center of the strips in the SB strips.

Conclusion

This study provides comprehensive insights into host associated microbiome assembly in strip fields with contrasting crops, disclosing the above and belowground dynamics within and across FB and SB strips. Our findings reveal considerable knowledge that will facilitate the thorough unravelling of crop field-level microbiome assembly, and harnessing microbiome-mediated benefits via optimal cropping systems design for sustainable crop production.

Keywords: diverse cropping system, barley microbiome, faba bean microbiome, plant neighbour effect, fungal pathogen dynamics, soil microbiome, phyllosphere microbiome

Introduction

Diversified cropping systems including intercropping and strip cropping, where two or more crops are co-cultivated on a parcel of land have generally been shown to be highly productive and resilient to biotic and abiotic stresses compared to monocropped systems [1–3]. Enhanced agronomic and environmental benefits characterizing diversified cropping systems minimizes agrochemical use [4] while maintaining high crop yields and production [5,6]. Accumulating evidence suggests that these diversified cropping-derived benefits could be driven by distinct microbial communities associating with the plants (collectively referred to as the plant-associated microbiome) [7–9]. The plant-associated microbiota plays a vital role in promoting plant growth via aiding in nutrient acquisition [10,11], disease suppression [12,13] and improving overall soil health [14]. While technological advancements and high-throughput omics techniques are enhancing our understanding of plant-associated

59 microbiota, the detailed mechanisms underlying plant-microbiota interactions for sustainable
60 crop production remain to be fully uncovered.

61 Agricultural fields are highly heterogenous with uneven distribution of microorganisms, that
62 are continuously affected by both host plants and environmental factors. Crop genotypes
63 harbour distinct associated microbiomes at differing microhabitats and strongly affect
64 microbiome dynamics and assembly. Belowground, soil physicochemical properties including
65 pH, organic matter, soil aggregate and nutrient status [15], and plant factors such as exudates
66 are the main factors driving the assembly of the host associated microbiomes [16–19]. The
67 phyllosphere microbiome is highly dynamic and is strongly influenced by environmental
68 factors, in this case wind, rain, ultraviolet radiation and temperature, as well as the
69 phenotypic characteristics of the host plant [20–24]. While environmental factors may drive
70 plant microbiomes at macroscale, host phenotypic characteristics have the strongest effects
71 at the microscale [20,23,25,26]. Morella *et al.*, (2020) [27] reported a strong habitat and host
72 genotype-dependent selection of plant-associated microbiomes using successive passaging
73 experimental setups. Comparatively, the soil microbiota is relatively stable, with soil bacteria
74 displaying lesser mobility than fungi, which are able to spread through hyphal networks in the
75 soil [28,29]. However, detailed empirical studies are still needed to establish microbiome
76 patterns and biogeography at the microscale in diverse cropping systems.

77 In mixed vegetations, plant microbiome assembly and their functions are affected by the
78 neighbouring plants, both below and above ground [30,31]. Plant neighbour effects on
79 microbiomes becomes stronger with increasing biomass than the reference host effects on
80 the host phyllosphere bacterial communities in the long term [31]. Different plant genotypes
81 host ecologically distinct microbiomes with potentially distinct functions. Thus, the effects of
82 plant neighbour could underline the amplified benefits derived from host-associated
83 microbiota, including enhancing nutrients acquisition, diseases suppression, and soil
84 biodiversity in diversified cropping systems compared to monocrop systems [32,33]. For
85 example, maize-peanut intercropping was reported to increase the nitrogen content of the
86 intercropped maize and alter the composition and diversity of the microbial communities in
87 the rhizosphere soil, including enrichment of beneficial microbes [34]. Plant neighbours have
88 also been reported to modulate microbial pathogen dynamics for example, by either reducing
89 or increasing fungal root pathogen *Rhizoctonia solani* attack of the focal plant [35]. Similarly,

this work also found that older plant neighbours reduced *Rhizoctonia solani* infection through delayed onset of transmission [35]. Additionally, heterospecific neighbor plants in intercropping systems (two or more crops grown together) or strip intercropping systems (where crops are sown in narrow strips for ecological interaction) [36,37], may serve as an additional source of microbiota for the plant. Locally dispersed microbiomes from neighbouring plants is an important source affecting phyllosphere assembly, and similarly, neighbouring plant genotype, biomass or age could strongly affect microbiomes of the host [31].

Studies investigating plant-associated microbiomes are mostly performed in pure stands. Thus, we have limited insights of plant microbiome composition, diversity and potential functions in diversified cropping systems. Also, effects of plant neighbours on the dynamics of the host microbiome are rarely investigated. Hence, empirical studies of plant microbiomes including the effects of plant neighbour on community structuring and diversity in strip cropping fields could disclose microbiota signatures and patterns that promote crop health, soil biodiversity, and ecosystem stability.

The aim of this study was to investigate the effects of strip cropping on microbial dynamics, including pathogens, below- and above-ground. We hypothesize that microbial community structure patterns and dynamics are spatially distinct within stripcrop fields and are strongly affected by contrasting crop type in the adjacent strips. The specific objectives include i) characterizing microbial diversity and composition of soil and leaf-associated microbiomes within specific locations within strips across different time points ii) assessing how specific microbial pathogens are distributed within the strip cropped-field and to iii) examine microbial co-occurrence network dynamics within the strip gradients.

Materials and methods

Experimental field design and management

A strip cropping fieldwas established in 2021 at the Sofiehøj experimental station, Denmark (Coordinates: 54.703353558133315°, 11.445337737133025°), with soils consisting of approximately 16% clay, 13% loam, 69% sand. Faba bean, spring barley, spring wheat, sugar beet, quinoa, rye, xx, xx and xx were grown in strips, and the position of each crop type in the field was rotated annually. In this study, we focus exclusively on faba bean and spring barley

strips. These strips were located adjacent to each other and replicated four times 60 m apart. The strips were 96-180 m long and 6 m wide (**Figure 1A;** Supplementary **Table S1**). The strip fields were cultivated with spring wheat and sugar beet in Month, 2021, and rotated with SB and FB, respectively in Month, 2022 and Month, 2023 (Supplementary **Table S1**). The experimental field layout is outlined in **Figure 1B.** Sowing was done in rows within each strips at X cm and X cm distance, respectively for SB and FB. Strips were maintained with manual weeding, watering and organic slurry applied to the SB plots seasonally, and additionally supplemented with an organic fertilizer, Øgro 10-3-1 in 2022 and 2023 (Supplementary **Table S1**). Øgro 10-3-1 is a 100% recycled organic fertilizer (10% total N, of which approximately 10% is NH_4^+-N) and soil conditioner for grains and other crops (https://www.oegro.dk/produkter/produktoversigt/oegro-10-3-1/).

Soil and shoot sampling

Soil and shoot samples were taken from the FB and SB strips in 2022 (at 2 weeks interval on 18 May, 02 June and 21 June) and in 2023 (at 3 weeks interval on 23 May, 14 June, and 06 July) (**Figure 1B**). Shoot samples were taken in every second row (designated E, C and A) starting from the edge and moving into the center of the strip, along a 10 m range in the row by randomly collecting leaves (5 and 3 leaves respectively for SB and FB, just below the flag leaf f/plant) from 10 plants (**Figure 1B**). Similarly, 5 soil samples (each consisting of a pool of 10 samples) were taken between the rows in a gradient from the edge of the strip and inwards to the center (E, D, C, B, A). Soil samples were collected at a depth of approximately 20 cm using a soil auger (2 cm diameter).

In 2022, we collected a total of 48 shoot samples (i.e. 2 crop species x 3 gradient positions x 2 sampling times x 4 replicates) and 120 soil samples (i.e. 2 crop species x 5 gradient positions x 3 sampling times x 4 replicates). In 2023, we collected samples at 5 sampling gradient positions each for soils and shoots, thus resulting in a total of 120 shoot samples (i.e. 2 genotypes x 5 gradient positions x 3 sampling times x 4 replicates) and a total of 120 soil samples (i.e. 2 genotypes x 5 gradient positions x 3 sampling times x 4 replicates). The collected samples were placed in labeled plastic bags and immediately kept in cold containers until later storage at -20 °C prior to DNA extraction.

DNA extraction

Shoot and soil samples were homogenized, followed by lyophilization for 72 h and ground using sterile steel beads (5 mm, Qiagen, Hilden, Germany) in a Geno/Grinder2000 at 1500

rpm for 3 × 30 s. We used 250 mg of each sample for DNA extraction. Shoot DNA was extracted using the DNeasy Plant Mini kit (Qiagen, Hilden, Germany) while soil DNA was extracted using the PowerLyzer™ PowerSoil® DNA Isolation Kit (Mo Bio Laboratories, Carlsbad, CA, USA), according to the manufacturer's instructions. DNA concentration was confirmed with Qubit dsDNA HS (High Sensitivity) Assay Kit (Invitrogen, Thermo Fisher Scientific). DNA samples were stored at − 20 °C until used for amplicon library preparation.

Library preparation and amplicon sequencing

The bacterial amplicon library were generated by amplifying 16S rRNA V5-V7 with 799F/1193R primer pairs [38–40]. The PCR reaction was performed in a 25 µl reaction mix consisting of 12.5 µl Invitrogen Platinum SuperFi PCR master mix (Thermo Fisher Scientific, Waltham, Massachusetts), 2 µl of each primer (10 µM stock), and 6.5 µl nuclease free water, and 2 µl of the template DNA. PCR amplification was performed in a GeneAmp PCR System 9700 thermal cycler (Thermo Fisher Scientific) using the following conditions: 94.0°C for 3 min, 35 cycles at 94°C 1 min, 55°C 1 min, 72°C 1 min, and a final extension step at 72 °C for 10 min. The fungal amplicon library was prepared using the fITS7 and ITS4 [41,42] fungal primer pair that amplify the internal transcribed spacer 2 (ITS2) region of the fungal rRNA gene [41]. The amplification was done in a reaction mixture of 25 µl as described for bacteria reactions. The PCR thermal cycling conditions for the fungal PCR was 94.0°C for 5 min, 35 cycles at 94°C 30s, 57°C 30s, and a final extension step at 72°C for 30s. For both bacteria and fungal libraries, we used dual indexing in combination with internal barcodes to pool samples. The bacterial and fungal forward primers were tagged with varying bases of multiplex identifiers [43,44]. For indexing, primers including indexing tags were used in a PCR with 10 cycles, with the thermal cycler programs as described above. PCR amplicon sizes of both bacteria and fungi libraries were confirmed on 1.5% agarose gel and expected band sizes excised and extracted using QIAquick Gel Extraction Kit (Qiagen). The libraries were sequenced on an Illumina MiSeq sequencer with PE300 at Eurofins MWG (Ebersberg, Germany).

Sequence data processing and statistical analysis

Bacterial and fungal sequences were analyzed using the DADA2 (v. 1.12) [45] in the R statistical package (R Core Team, Vienna, Austria). Briefly, the raw reads were quality filtered and trimmed (filterAndTrim - maxN = 0, maxEE = 2, truncQ = 2), followed by error learning (learnErrors), dereplication (derepFastq) and merging of forward and reverse reads

(mergePairs) prior to the construction of the sequence table (makeSequenceTable) and chimera removal (removeBimeraDenovo). Taxonomic assignment was done using the reference databases SILVA version 128 [46] and the UNITE database [47] train sets (https://benjjneb.github.io/dada2/training.html), for bacterial 16S rRNA and fungal ITS, respectively, using the implementation of the naive Bayesian classifier in dada2 R package. Unassigned ASVs at kingdom level and ASVs assigned to chloroplast or mitochondrial sequences were excluded from all the datasets.

Statistical analyses and visualizations were performed in R v3.3.0 [48] using vegan (v2.5.7) [49], phyloseq (v1.34.0.) [50], and ggplot2 (v3.3.2) [51] packages. The filtered data were normalized and used for visualizing microbial relative abundances in the samples. We examined significant differences in the relative abundances of specific pathogenic fungi using a two-group White's nonparametric t-test in the STAMP software v2.1.3 [52,53], with the Benjamini-Hochberg FDR to control for multiple testing [54]. We assessed alpha diversity (observed richness and Shannon diversity) and statistically significant differences using the non-parametric Kruskal–Wallis test followed by Bonferroni–Dunn multiple comparison test between groups. The ASV tables were transformed into relative abundances prior to beta diversity analysis. We visualized the Bray-Curtis dissimilarity matrices using unconstrained principal coordinates analysis (PCoA). Following, we perfoemd Permutation analysis of variance (PERMANOVA) statistical tests to determine the effects of experimental factors on the community dissimilarity using "adonis" in the vegan package, with 1000 permutations. Pairwise comparison was performed to assess differences between microbial communities across the sampling gradients using the pairwiseAdonis function (https://github.com/pmartinezarbizu/pairwiseAdonis).

We quantified soil edaphic parameters in the strips and test for significant differences using the cal_diff (method = anova) and plot_diff functions within the trans_env function in the R package "microeco" [55]. Additionally, we performed redundancy analysis (RDA) and Pearson correlation analysis to evaluate the relationships between microbial communities and soil physicochemical properties, using the microeco package.

In addition, indicator species analysis [56] was performed to identify microbial ASVs which were significantly associating with specific sampling gradient positions using the indval function in the labdsv package [57]. We used splitted shoot and soil data for SB and FB samples

for this analysis. Significant bacterial ASVs (bASVs) and fungal ASVs (fASVs) were defined as those with $p < 0.01$ and an indicator value of at least 0.4. We further assessed the functional potential associated with the identified indicators. Bacterial and fungal functional profile were predicted with the functional annotation of prokaryotic taxa (FAPROTAX) [58] and FungalTraits [59], respectively, using the microeco' package [55].

Correlation analysis and microbial co-occurrence networks

We constructed gradient specific microbial co-occurrence networks as described previously [12], to explore interactions between specific microbial taxa at specific gradient positions in shoot and soil of FB and SB. Briefly, we combined bacterial and fungal datasets and normalized it using the trimmed mean of M values (TMM) method using the package EdgeR [60]. Correlation analysis was performed using ASVs that were present in at least 10 samples with Spearman's rank correlations > 0.4 for positive correlations and <-0.4 for negative correlations, with $p < 0.05$, and correction using Benjamini-Hochberg FDR. Significant correlations were visualized at the genus level using heatmaps. Next, we constructed microbial co-occurrence networks at the phyla level with ASVs set as nodes and correlations as edges. Network metrics such as transitivity or clustering coefficient (the probability that the adjacent nodes of a node are connected), mean degree (the average number of edges across all nodes in a network), density (fraction of all possible edges actually realized), average path length (APL) (average number of steps which would be required to reach from one node to another in the network) and modularity (measures how well the network is organized into distinct modules) were computed, using the "igraph" package [61]". Furthermore, we computed the hub or keystone taxa representing the top 5% of the ASVs with the most correlations in each of the constructed networks. Highly connected ASVs were identified and their relative abundances across were visualized.

To examine whether community resilience differ between sampling sites within strips, we assess the robustness of each co-occurrence network based on network attack tolerance strategies using the NetSwan package for R [https:// cran.r-project.org/web/packages/NetSwan/index.html]. Each location specific network was assessed using four attack to vulnerability strategies involving systematic node removal using four strategies. These strategies included (i) random removal, (ii) direct removal, where nodes were removed in descending order of their BNC (betweenness centrality) value (i.e., number

of times a node is found on the shortest path between other nodes), (iii) targeted on nodes with the highest impact closeness (degree), and (iv) cascading removal, involving the recalculation of BNC values after each node was removed. The effect of each attack metric on network stability was visualized using connectivity loss as a function of fraction of nodes removed.

Results

Sequence data summary

For characterizing the effects on microbial diversity of strip cropping, we sampled soil and shoot samples of SB and FB across spatial gradients from the edge of the strip (close to the neighbouring crop) towards the centre of the strips at three different timepoints in 2022 and 2023. Sequence reads from the soil and shoot bacterial and fungal samples, with read numbers and sequences read statistics in both 2022 and 2023 are summarized in **supplementary file Table S2,3**. We did not analyse the bacterial reads from the shoot samples collected in 2022 due to poor quality and they were thus removed from the dataset.

Microbiome composition, diversity and indicators in strip fields in 2022

Shoot bacterial relative abundance were highly distinct across the gradients of the strips of FB and SB (**Figure 2A)**. For example, the bacterial genus *Rosenbergiella* was highly enriched in the centre of the strips in FB, while the bacterial family Enterobacterales was significantly enriched in the center (A and C) compared with the edge (E) (**Supplementary Figure S1A,B**). In contrast, Afipia, Mesorhizobium, Siccibacter and Pantoea were highly enriched in the edges of the strips (E) (Figure 2A, **Supplementary Figure S1A,B**). In the SB shoots, Pseudomonas and Burkholderia were decreasing from the center towards the edge, while Staphylococcus had a contrasting trend (Figure 2A, **Supplementary Figure S1C**). We observed contrasting shoot bacterial alpha diversity trends in the two crops with a decreasing richness from the centre towards the edge in FB, whereas the highest alpha diversity was at the edge in SB and decreasing towards the centre (**Figure 2B**). However, the bacterial richness in SB shoot was only significantly ($p<0.05$) higher in the centre location (A) compared with the edge (E) (**Supplementary Table S4**).

Shoot bacterial community composition was clearly distinct along the gradients in both FB and SB (**Figure 2C,D**) as also confirmed by PERMANOVA (**FB: Adonis, R^2 = 0.48; SB: Adonis, R^2**

= 0.49, P<0.01; Supplementary Table S5). Pairwise PERMANOVA comparisons revealed significant differences within the gradients (**Supplementary Table S5**).

In soil, bacterial relative abundances were similar across gradients and time in both FB and SB (**Supplementary Figure S2**), while alpha and beta diversities were distinct across gradients (**Supplementary results, Figure S3-4 and Table S5**).

Indicator species analysis revealed unique clustering of specific bacterial taxa in the individual gradient positions within the strips of both shoot of FB and SB (**Figure 2E,F**). Specifically, bacterial genera *Afipia*, *Pantoea*, *Sphingomonas* and *Bradyrhizobium* were distinct indicators for the edge of the strips in FB (**Figure 2E**). The genera *Pseudomonas* and *Sphingomonas* strongly associated with the centre of the strips (A,C) while *Staphylococcus* and *Exiguobacterium* were main indicators of the strip edges of SB (**Figure 2F**). Unlike the shoot gradients, indicator bacterial taxa were fewer and rarely distinct across the gradients of the strips (**Supplementary Table S4B**).

Relative abundances of fungi in shoots were distinct across the gradients (**Figure 3A**). Most remarkably, in SB, the fungal genus *Puccinia*, containing the pathogen *Puccinia hordei*, was steeply decreasing from the centre towards the edge of the strips at sampling time 2 while this gradient had disappeared at sampling time 3 (**Figure 3A,B**). Similarly, at the earliest sampling time, other potential pathogenic taxa in shoots including *Ramularia* and *Cladosporium* differed significantly in relative abundances at different sampling gradient positions of SB (**Figure 3B**). *Cladosporium* and *Holtermanniella* decreased, while *Vishniacozyma* and *Dioszegia* were increased from the centre towards the edge of strips in FB at sampling time 2. In contrast, soil fungal relative abundances were similar across the gradients within SB and FB (**Supplementary Figure S6)**. Because there was an overlap in the ASVs occurring in the phyllosphere and rhizosphere, we further assessed the fungal pathogens dynamics in the soil and found that *Cladosporium* and *Fusarium* were significantly different between soils samples from the centre and edge locations at sampling time 1 and time 2 (**Supplementary Figure S7,8**).

Generally, shoot fungal alpha diversity was distinct, with fungal Shannon diversity declining from centre to edge in both SB and FB at T2, but the opposite trend appeared at T3. **Figure 3C, Supplementary Table S6**). Shoot fungal beta diversity clearly separated the fungal

communities across the spatial gradients in both FB and SB (**Figure 3D**). PERMANOVA confirmed the significant effect of the gradient position on shoot fungal communities in FB (sampling time 2; **Adonis, R^2 = 0.47,** Sampling time 3, **Adonis, R^2 = 0.43, P< 0.001, Supplementary Table S5**) and SB (sampling time 2; **Adonis, R^2 = 0.42, P< 0.001,** Sampling time 3, **Adonis, R^2 = 0.33, P<0.05** (**Supplementary Table S5**). Further pairwise tests revealed significant differences in shoot fungal communities within the gradients (**Supplementary Table S5**).

Soil fungal alpha diversity was rarely distinct across site (**Supplementary Figure S9, Table S7)** but community composition markedly clustered for specific gradient positions in both FB in SB (**Supplementary Figure 10)**. The gradient effect was consistently significant in SB (Sampling time 1, **Adonis, R^2 = 0.36, P< 0.01,** Sampling time 2, **Adonis, R^2 = 0.32, P< 0.01,** Sampling time 3, **Adonis, R^2 = 0.40, P< 0.001**) and further confirmed by pairwise test effects of sampling location (**Supplementary Table S5**). Additionally, we identified specific indicator fungal taxa associated with specific shoot and soil samples from different sampling gradients (**Figure 3 E, Supplementary Figure S11, 12**).

Microbiome composition, diversity and indicators in strips in 2023

Following rotational strips in 2023, we collected and analysed shoot and soil samples similarly as described for 2022. Distinct bacterial relative abundances were observed at different gradient positions, likewise a noticeable shift in these abundances at the different sampling times in both SB and FB (**Supplementary Figure S13)**. Generally, *Burkholderia* dominated the shoot bacterial community in both SB and FB at all sampling time. Soil bacterial relative abundance was similar across gradients and time (**Supplementary Figure S14A)**. The relative abundance of *Puccinia* was highest in the centre of the SB strips, confirming the observations in the 2022 dataset (**Figure 4A,B**). *Cladosporium* was significantly highest in the edges of the strips, while *Blumeria* was significantly enriched in the centres of the strips in SB (**Figure 4C**). In soil, fungal relative abundances were distinct between the SB and FB strips (**Supplementary Figure S14B)**, but similar across the gradients in the strips.

We analysed the proportion microbial taxa of that were present in shoot samples of both FB and SB. Shared shoot bacterial taxa were rarely different between gradient positions (**Supplementary Figure S15**). Generally, the strip edges (A) having the least distance between

FB and SB, had the highest number of shared fungal taxa (39%), followed by the next gradient position (C) (35%) and least within the centre positions (E) furthest apart (31.5%) (**Figure 4 D**). Microbial alpha diversity generally confirmed results in 2022 (**Supplementary Figure S16,17; Supplementary Table S8,9).**

Shoot bacterial community composition was markedly distinct across gradients of shoot and soil for both FB and SB, while in soil, sampling time affected microbial communities of both FB and SB, but these effects were stronger on fungi than bacterial communities (**Figures 5, Supplementary results**).

We found indicator species across strip gradients, displaying potential functions at different sites and at different time points in both soil and shoot SB and FB (**Supplementary Figure S19A,B; S20-24**). In SB shoots, bacterial functions assigned to fermentation and anaerobic chemoheterotrophy characterized the centre sampling location, while aerobic chemoheterotrophy was higher in the edge locations (**Supplementary Figure S20**). Similarly, we observed higher functions of dark hydrogen oxidation, nitrogen fixation, human pathogens, animal parasites, ureolysis in the edge sampling locations of FB shoots. In SB soil, functions associated with primary lifestyle mycoparasite, unspecified saprotroph and secondary lifestyles fungal decomposer, litter saprotroph and plant pathogen were significantly higher in the edge than the centre gradient (**Supplementary Figure S23**). Potential fungal functions like foliar endophytes and dung saprotroph were highly enrich in the centre than the site sites.

Gradient-specific correlation analysis identified distinct positive and negative interactions among microbial taxa in shoot and soil samples of FA and SB (**Figure 6A; Supplementary Figure S25**). A higher number of correlations were detected in shoots of SB than in FB. In shoot SB, the strip edges had the highest and most negative correlations. The genera *Siccibacter* and *Erwinia* negatively associated with *Puccinia* in centre sampling location A, while *Pantoea*, *Cupriavidus* and the order Enterobacterales also negatively correlated with *Puccinia* in the edge strip (**Figure 6A)**. Also, the genus *Burkholderia* correlated negatively with *Alternaria* in samples from the centre sampling location A and edge (E). Similarly, in FB shoot, *Pantoea* negatively correlated with *Alternaria* in centre location A, and similarly *Sphingomonas*, *Ralstonia*, *Burkholderia* and *Bradyrhizobium* (**Figure 6B)**. In soil, a higher number of negatively correlating taxa was found in centre gradients than the edge in FB, including the genus

Fusarium correlating with *Bacillus*, *Nitrospira*, *Nocardioides* and *Variovorax* (**Supplementary Figure S25**).

Gradient specific co-occurrence networks and resilience characterizing sampling locations in strip fields

Microbial co-occurrence networks revealed distinct patterns of microbial associations in the shoot and soil bacterial and fungal datasets at the three specific gradients within FB and SB (**Figure 7A,B**). Network node and edge numbers (both positive and negative) inferred from each network and additional network properties are summarized in the **Supplementary Table S11**. Overall, FB shoot networks were more densely connected than the SB shoot networks in the different gradient positions. SB shoot networks were the most distinct with highly sparse structure at the centre of the strip to more dense and highly connected networks towards the edge (**Figure 7A**). Network metrics including mean degree (Mn) and average path length (APL) corroborated the differences in co-occurrence networks across strip gradients in SB. Specifically, the mean degree of the SB shoot network was 7.07, 14.58 and 13.26 in locations A, C andE, respectively. Similarly, the APL was highest in networks of the centre of the strip and declined in networks at the edge (**Figure 7A**). FB shoot networks also revealed subtle differences in network properties with modularity being highest in the edge networks of both shoot and soil (**Figure 7B**). Furthermore, soil gradient specific networks were distinct between FB and SB (**Supplementary Figure S26**). We identified distinct number of hub taxa with varied connections and relative abundances in specific gradient networks (**Figure 7).** Fungal genera *Vishniacozyma* (species *V. victoriae*) and *Taphrina* were predominating hub taxa with high relative abundance in both FB and SB networks. *V. dimennae* and V. *victoriae* were highly abundant hub taxa in the edge network while *Taphrina*, *Sporobolomyces* (species *S. roseus*) and *Neosetophoma* dominated the centre networks of SB. In FB, bacterial genera *Burkholderia* dominated the centre, likewise *Papiliotrema* (species *P. flavescens*) which was also highly abundant at the edge. *Cladosporium* was the most abundant hub taxa in the edge networks of FB.

We tested the robustness of the networks by assessing their tolerance using four node sustained attack strategies, including random removal, direct removal of nodes with highest betweenness centrality, targeted on nodes with the highest impact closeness (degree), and an approach involving a combination of random and targeted on betweenness (cascading).

Among the tested strategies, random removal had the least connectivity loss, whereas degree and cascading attacks caused the lowest tolerance in both shoot and soil networks (**Figure 7A,B, Supplementary Figure S26**). SB shoot gradient specific networks exhibited a pronounced breakdown vulnerability which was higher in the centre network compared with edge networks when assessing breakdown with the all the attacking strategies, except degree attack (**Figure 7A)**. Removal of 50% nodes resulted in a 100% breakdown attacking degrees, compared with at least 60% nodes removal for a total disintegration in the other tolerance strategies. For the FB shoot gradient networks, a higher number of node removal (57%) is required to totally disrupt the networks, when using degree (for all networks), and for cascading and betweenness of locations A and E networks (**Figure 7B)**. Although subtle differences were observed between soil gradient specific networks, attack strategies did not reveal clear differences **Supplementary Figure S26A,B**).

Discussion

Mixed cropping systems have been well documented to promote high microbial biodiversity that have been suggested to enhance crop growth and disease suppression [7–9,62]. Plant associated microbiomes have been widely suggested as the “green solution” for sustainable crop production, primarily due to its multifaceted role in plant development [63]. Yet, we still have limited understanding of the effects mixed cropping systems such as strip cropping on microbiome composition, diversity and dynamics at the field scale. In the present study, we examined the effects of faba bean (FB) and spring barley (SB) neighbour plants on the contrasting hosts shoot and soil microbiomes across different time points. FB as a dicot belonging to the family Fabaceae and SB as monocot in the Poaceae family were expected to assembledistinct microbiomes that could affect plant performance within the respective strips. We also expected that microbiome assembly would depend on the presence of the adjacent crop, but to which extent the proximity to the adjacent crop would affect microbiome assembly above- and belowground was less predictable.

Microbial communities are dynamic and distinct across strip crop spatial gradients

We found distinct microbial communities in the spatial gradients within the SB and FB strips, thus confirming our hypothesis of neighbor-effects on the host-associated microbiomes in the strips.

We found that the phyllosphere communities were more distinct across the gradient of SB and FB at the early stages compared to the later stages, indicative of stronger effects of species effects at early stages and this become masked at later stages, primarily by environmental factors [68]. However, soil fungal communities were distinct at later stages suggesting stronger effect of the plant in structuring the fungal than bacterial communities. Both sampling time and gradient position significantly affected microbial community structures in shoot and soil of both FB and SB, except for soils in SB where gradient position did not affect the bacterial community significantly. Sampling time contributed the highest effects on microbial communities suggest effects of continuous confounding host physiological changes [69–71].

Our data clearly revealed a more dynamic shoot microbiota in SB compared to FB, further corroborating the effects of distinct host phenotypic traits on microbial community assembly [23]. While limited work exists comparing microbiome assembly in shoots of monocot and dicots, reports show that broadleaved woods hosted higher proportions of N-fixing bacteria [72]. Leaf type, surface microtopography and canopy cover determines surface area for microbial colonization and affect micro-environmental factors (temperature, relative humidity, wind) differentially affecting microbial communities [23]. Although we did not quantify nutrients in SB and FB, monocots and dicots accumulate varying levels of leaf nutrients such as N and P [73], that might drive distinct microbial community assembly [74]. Sangiorgio *et al.*, (2024) [74] reported that foliar C:N ratio contributed to the difference in phyllosphere bacterial communities across sites in Scots pine. Also, the highly dynamic and consistent shoot microbiomes observed compared to soil of SB and FB samples in 2022 and 2023 is not surprising as highly perturbating weather factors strongly alter the phyllosphere microbiome [75]. Almario *et al.*, (2022) [68] reported reproducible dynamics and patterns of shoot microbiomes throughout the growing season. Furthermore, microbial community structures were distinct in FB and SB, supporting previous studies of species effects on plant-associated microbiomes [12,43].

Specific fungal pathogens were distinctively distributed within strips

Strip cropping systems have been suggested as a sustainable way of reducing pathogen pressures. We found that the relative abundance of potential plant fungal pathogenic genera on SB shoots, specifically *Puccina* was consistently higher in the centre than at the edge strips of at earlier sampling time in both 2022 and 2023. These results were consistent in the

individual replicated samples across the field, thus providing strong evidence of *Puccinia* development in the centre of the strips. The genus *Puccina* contains *Puccinia hordei* causing the destructive leaf rust disease of cereals globally [76]. Other fungal pathogenic genera, including *Blumeria* (causing powdery mildew), *Ramularia* (causing leaf spot) and *Cladosporium* (causing leaf spot, scab, and blights), were also found to be differentially distributed along the gradient in both 2022 and 2023. Similarly, profiling of these pathogens in soil revealed consistent enrichment of *Cladosporium* in the centre location, while *Fusarium* was enriched at the edge. These findings suggest differing tendencies of fungal pathogenic attack at specific sites within strip fields, as previously reported [77]. Further, we speculate that incidence of shoot diseases such as those caused by *Puccinia* and soil diseases caused by *Fusarium* species could occur in the centre and edges, respectively, within SB strips. Whether the microbiota sourced from neighbour plants affects the spread of pathogens would require further studies with varying strip field design. However, there is evidence that root-exuded metabolites of neighbour plants regulates plant susceptibility to soil pathogens in intraspecific mixtures [78]. Similarly, pathogen suppressive volatiles from neighbour plants could result in reduced leaf or root pathogen establishment in a strip cropping system [10][79]. Repeated strip rotation with crops secreting bioactive root exudates could induce soil suppressiveness against microbial pathogens. Moreover, it is interesting to note that pathogenic lifestyles may be plant type dependent, as a pathogen of dicots could eventually act as a biocontrol agent in a monocot plant [80].

Indicator species across strip gradients with potential functions

We identified indicator microbial taxa that were associated with either the centres or the edges of the strips. For instance, at timepoint three in 2022, the bacterial indicators *Afipia*, *Pantoea*, *Sphingomonas* and *Bradyrhizobium* were associated with edges of the FB strips. In the SB strips, Pseudomonas and *Sphingomonas* associated with the centres, while *Staphylococcus* and *Exiguobacterium* were main indicators of the edges in the strips of SB. Several of these taxa have profound beneficial roles for the plant host and thus have been studied for their biocontrol traits [81]. For example, *Pantoea agglomerans* has a strong antagonistic effect against a wide range of pathogens in many plant species (reviewed in [82]. Functional analysis based on microbial taxonomic data could reveal insights for understanding

potential functional traits for promoting applications for sustainable agriculture [83]. Furthermore, we show site-specific functional attributes associated with these indicator species identified in above and below-ground, in both strip fields, and is indicative of microhabitat effects on microbial functions and distributions. These findings further extend the potential effects of neighbouring plants beyond community diversity to influencing microbial functional traits and distribution across strip fields. A recent study also found that core microbial taxa distributed in multiple wheat microhabitats significant correlated with soil functional traits, as well as soil variables and crop productivity [66].

Interspecific neighbour effect is gradient-dependent across adjacent strips

Current knowledge of plant species or genotypic effects on the associated microbiomes is still largely based on the intricate interactions between the focal plant and the microbiota, with limited consideration of potential neighbour specific effects on microbiome assembly on the focal plant. We found a higher number of shared shoot fungal genera in the samples taken close to neighboring strips compared to the samples taken more distantly from the neighboring strips. However, we identified a shared shoot bacterial genera between SB and FB strips, demonstrating a stronger interactive effect of neighbouring crops on the shoot mycobiome. It has been shown that plant neighbour effects become stronger over time with increasing microbiota dispersal from neighboring plants as plant biomass increases [31]. This neighbour effect might eventually decrease host filtering effects on bacterial communities over time [31]. We speculate that the shared microbial taxa emanating from the adjacent neighbours could be affecting overall host performance. For instance, beneficial microbial species acquired from the neighbouring plant could be antagonizing pathogenic microbes on the focal plant. Further experimental evidence is needed to assess how the newly arrived microbiota from neighbouring crops affects focal host-microbial pathogen interactions in strip crop systems.

Distinct gradient-specific microbial interactions and co-occurrence networking within strips

Although, correlation-based analysis does not demonstrate cause and effect, it enables us to discern into plausible ecological relationships between microbial species, and between microbes and the environment [84]. Thus, we further examined whether microbial co-

occurrence patterns characterize gradient positions using correlation-based analysis and network visualization. Positive and negative correlations suggested potential positive and antagonistic interactions, respectively, within the host associated microbiota [29]. Correlations at lower taxa level revealed distinct associations with *Siccibacter* and *Erwinia* negatively correlating with *Puccinia* in the centre site A, while *Pantoea* and *Cupriavidus* also negatively correlated with *Puccinia* in the edge strip of SB. Erwinia species have been shown to suppress *Puccinia recondite* [85] causing wheat leaf rust [86], and *Siccibacter colletis* was reported to promote wheat growth via enhancing phosphate and potassium uptake [87]. Similarly, *Pantoea* species are notable known for their biocontrol activities against several pathogenic microbes attacking different plants species [82]. Thus, the varying microbial correlations associated with specific gradient positions in strips support the localized microbial interactions that could affect microbiome modulating effects on plant functions.

As expected, inter-phylum co-occurrencenetworks exhibited a more dissimilar configuration in the shoots than in the soil, primarily due to higher dynamic patterns of the phyllosphere microbiota. Also, shoot networks varied more across the gradient in SB compared than in FB , thus corroborating the distinct community dynamics in grasses and broad leaf plants. In SB, shoot networks showed greater microbial community connectivity and robustness to disturbances at the edge than in the centre. The network metrics corroborate the dissimilar microbial co-occurrence interaction. These metrics also reveal insights into the microbial community dynamics during external perturbations. For instance, the transitivity and low APL characterizing the SB edge network indicate a more connected and robust network [13] compared with the centre networks. The robust SB edge network could suggest stronger microbial competition [88], which could further enhance resistance to pathogen attack. While FB shoot networks were quite similar, the high modularity characterizing edge networks suggests higher invasion rates of these communities [89,90]. However, detailed studies are needed to validate the biological relevance of these interactions at individual gradient positions.

We found hub taxa with different occurrences along the strip gradients indicative of the distinct role of specific microbial taxa in community structuring. Keystone taxa are known to modulate several functions, which include regulating the invasion of fungal pathogens [91]. *Sporobolomyces roseus*, dominant hub taxon at the centre position of SB has been reported

to be antagonistic via nutrient competition against *Botrytis cinerea,* the causal agent of grey mold disease [92], and against *Cochliobolus sativus* [93] that causes several diseases in cereal crops, including spot blotch and common root rot [94]. Moreover, *Vishniacozyma victoriae*, a hub taxa in both SB and FB networks is suppressive against *Botrytis cinerea* [95,96], and *Penicillium expansum,* and *Cladosporium sp.*, [96]. Also, *Papiliotrema flavescens*, a dominant hub taxon at the edge of FB strips have notable plant growth-promoting properties including induction of systemic resistance against *Botrytis cinerea* in *Arabidopsis* [97]. Additionally, the bacterial genus *Burkholderia* is known for biocontrol traits against a wide range of plant pathogens [98]. Altogether, these results demonstrate that keystone species spatially distributed within strips could be driving microscale cooccurrence community interactions.

Network tolerance to disturbance confirms the higher robustness of edge than the centre shoot networks of SB. Networks with higher robustness are able to resist rapid collapse caused by disturbance, for example pathogen attack [13], and thus have greater stability [99]. Thus, these results suggest that stronger resilience is associated with strip edge than strip centre shoot networks, and as such the centre of the strips is expected to be more vulnerable to pathogen attack compared with the edge of the strips. Interestingly, these results support the higher negative correlations detected at the edge location, likewise a higher effect of neighbour revealed in the number of shared microbial taxa. However, the larger gradient-specific variation in the SB compared with the FB suggest that community resilience within strips is dependent on the host type. Moreover, since networks are dynamic due to the continuous influence of neighbour host and environmental factors [99], the observed site-specific microbial co-occurrences would change across time, and would correspondingly, alter resilience patterns within strip-crop fields.

Conclusions

The present work investigated the dynamics and site-specific assembly of soil and phyllosphere microbiomes in a rotational faba bean (*Vicia faba*) and spring barley (*Hordeum vulgare*) strip field during two years using amplicon sequencing. We found distinct microbial composition, community structure and specific potential functions characterizing both above and belowground sampling locations within and between strips with spring barley and faba bean. Relative abundances of fungal pathogens, such as the genera *Puccinia*, *Blumeria* and *Cladosporium* varied across strip gradients, specifically, *Puccinia* was consistently enriched in

the centre of the strips compared with the edges in SB. Moreover, neighbouring strips has higher effects on the microbial richness in the plants that were closest to the edges. Additionally, we revealed distinct site-specific microbial interactions and co-occurrence networking within strips. Inter-phylum shoot co-occurrence networks exhibited more dissimilar network configurations compared with the soil networks, primarily due to more dynamic patterns of the phyllosphere microbiota in SB. Network tolerance to disturbance confirms more resilient networks at edges than centres in the SB strips. The distinct microbial cooccurrences exemplified by network structure, topology and hub taxa could explain varying community resilience that characterize strips with different crops and sites within strips. Altogether, these findings reveal in depth knowledge that will facilitate the thorough dissection of crop field-level microbiome assembly and further, generating mixed-host mechanistic hypotheses of microbiome dynamics positively promoting sustainable cropping systems.

Acknowledgements

We thank Louise Reinbach Rasmussen and Simone Ena Rasmussen for their excellent laboratory assistance.

Author contributions

MN, MV, ON and ENK planned the study. ON designed the strip field experiment. ENK, MV MTG and MN collected samples from the field. ENK analyzed the data and drafted the initial manuscript. All authors have read, revised, and approved of the manuscript.

Funding

The work was funded by GUDP Organic RDD6 project number 34009-20-1703.

Data availability

The MiSeq paired end reads obtained from the bacterial 16S rRNA gene (V3- V4) and fungal ITS2 gene regions have been deposited in NCBI SRA repository, under BioProject ID xxxxx and Submission IDs:xxxxxxxxxxxx

Declarations

Ethical approval and consent to participate Not applicable.

Consent for publication

Not applicable.

Competing interests

The authors declare no competing interests.

ORCID

Enoch Narh Kudjordjie
https://orcid.org/0000-0002-3297-2459
Mette Vestergård
https://orcid.org/0000-0002-0054-4855
Mesfin

Otto Nielsen
Mogens Nicolaisen
https://orcid.org/0000-0002-0407-2488

List of tables

Table 1: Summary of permutational analysis of variance (PERMANOVA) using the "adonis" test on Bray-Curtis distance matrices using bacterial and fungal community dissimilarity assessment using 1,000 permutations using 2023 dataset.

Dataset	**Compartment**	**Factor**	**Bacteria (16S) R^2**	**Fungi (ITS) R^2**
Faba bean (FB)	shoot	Sampling location	0.06**	0.07**
		Sampling time	0.56***	0.43***
		Sampling location x Sampling time	0.13***	0.14***

	Soil	Sampling location	0.10**	0.09**
		Sampling time	0.05*	0.18***
		Sampling location x Sampling time	0.18**	0.18*
Spring barley (SB)	shoot	Sampling location	0.06*	0.06**
		Sampling time	0.62***	0.48***
		Sampling location x Sampling time	0.09***	0.13***
	Soil	Sampling location	ns	0.11***
		Sampling time	0.07*	0.23***
		Sampling location x Sampling time	ns	0.19***

Significance of test indicated as ***, p <0.001; **, p <0.01; *, p <0.05. The ns denotes not statistically significant and R^2 is the proportion of variation explained.

List of figures

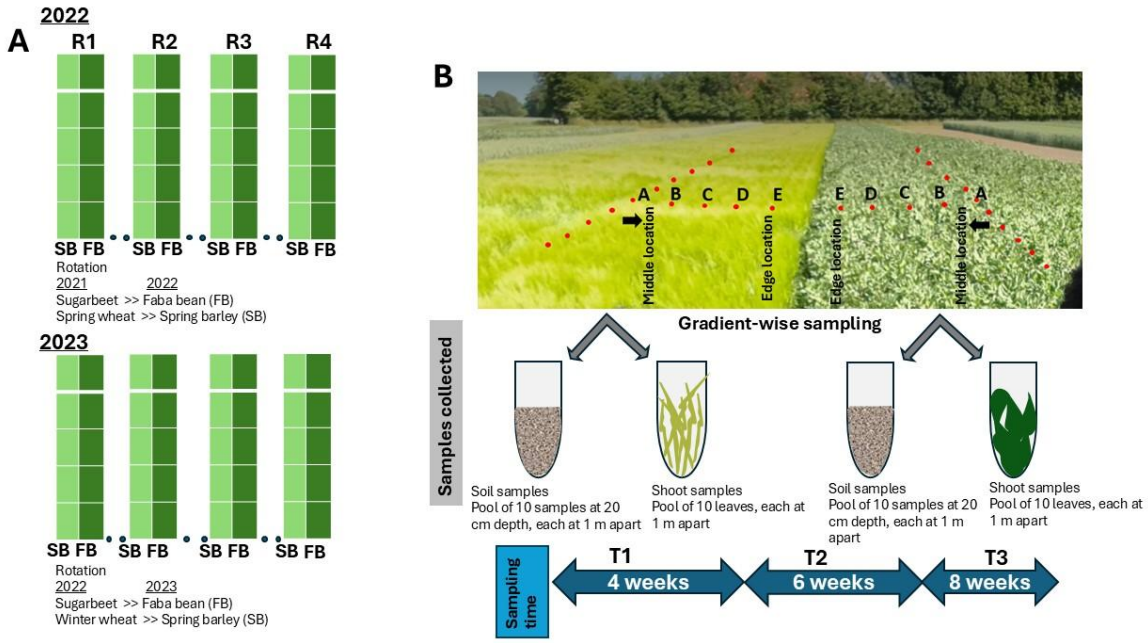

Figure 1.

Figure 1. Overview of experimental FB-SB field design and sampling. A) Scheme of spring barley (SB) and faba bean (FB) in strip layout including field replication at 60 m apart. Crops cultivated prior to FB and SB in the respective years are also indicated. B) Snapshot of strip field showing soil and shoot sampling (in red dots) across strip gradient, and time interval of

sampling.

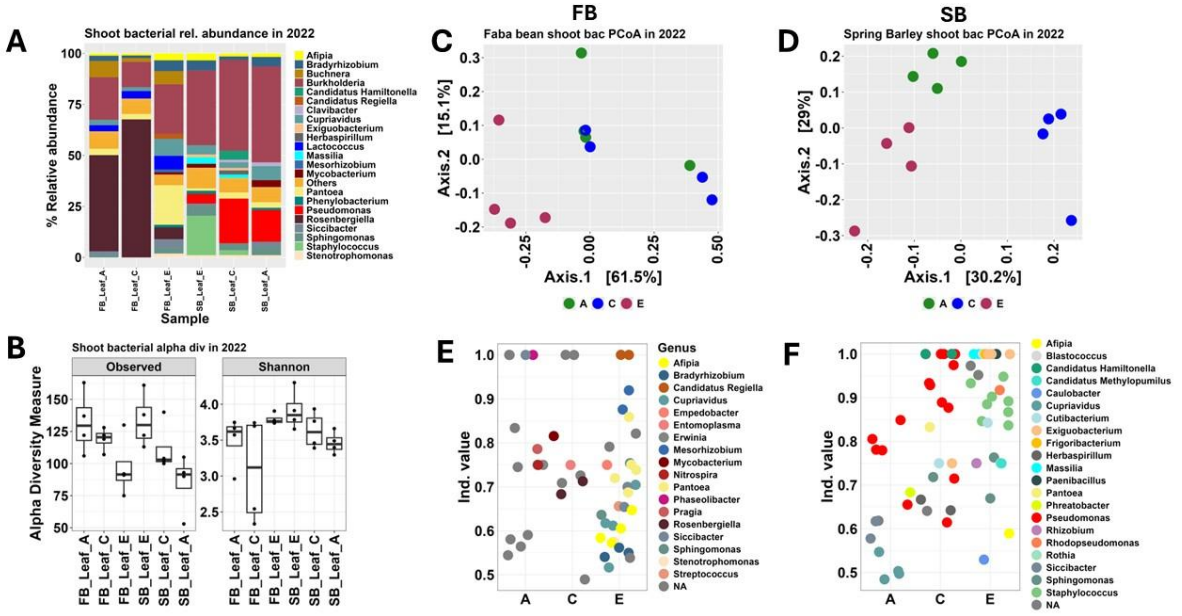

Figure 2.

639

640 **Figure 2.** Shoot bacterial communities within and across FB and SB strips in 2022. A) Bacterial
641 relative abundances B) alpha diversity C) and D) PCoA, E) and F) indicator species in FB and SB
642 shoot samples collected in from centre of strip towards the edge border rows.

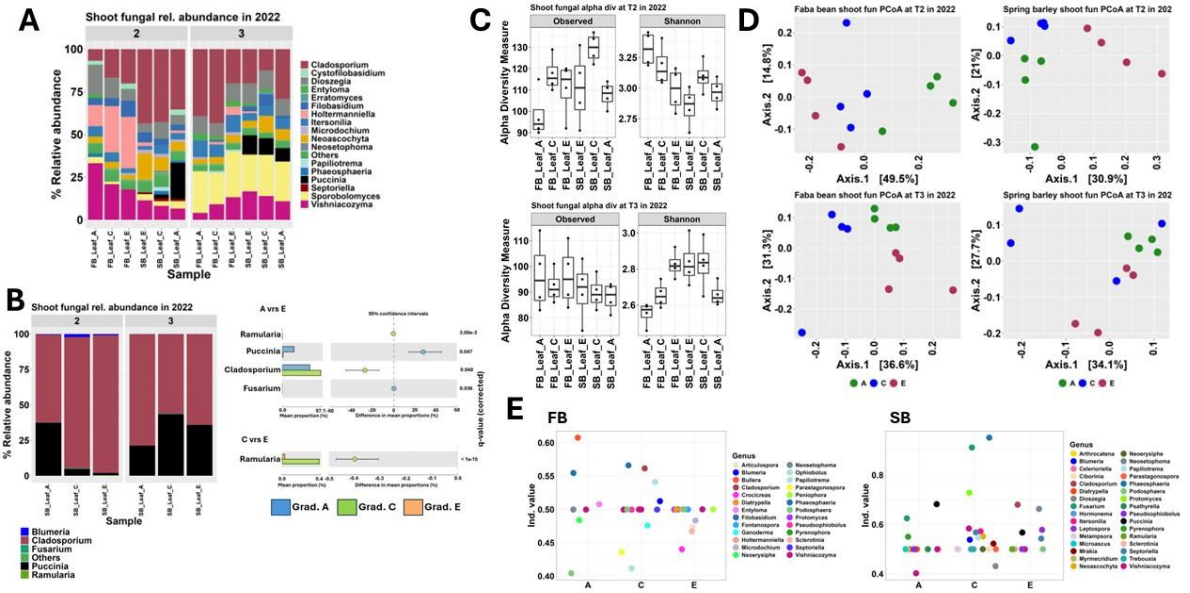

Figure 3.

643

644 **Figure 3.** Shoot fungal communities within and across FB and SB strips in 2022. A) Bacterial
645 relative abundances, B) relative abundances of potential fungal pathogenic taxa in SB, C) alpha

diversity, D) PCoA and E) indicator species in FB and SB shoot samples collected from centre of strip towards the edge rows.

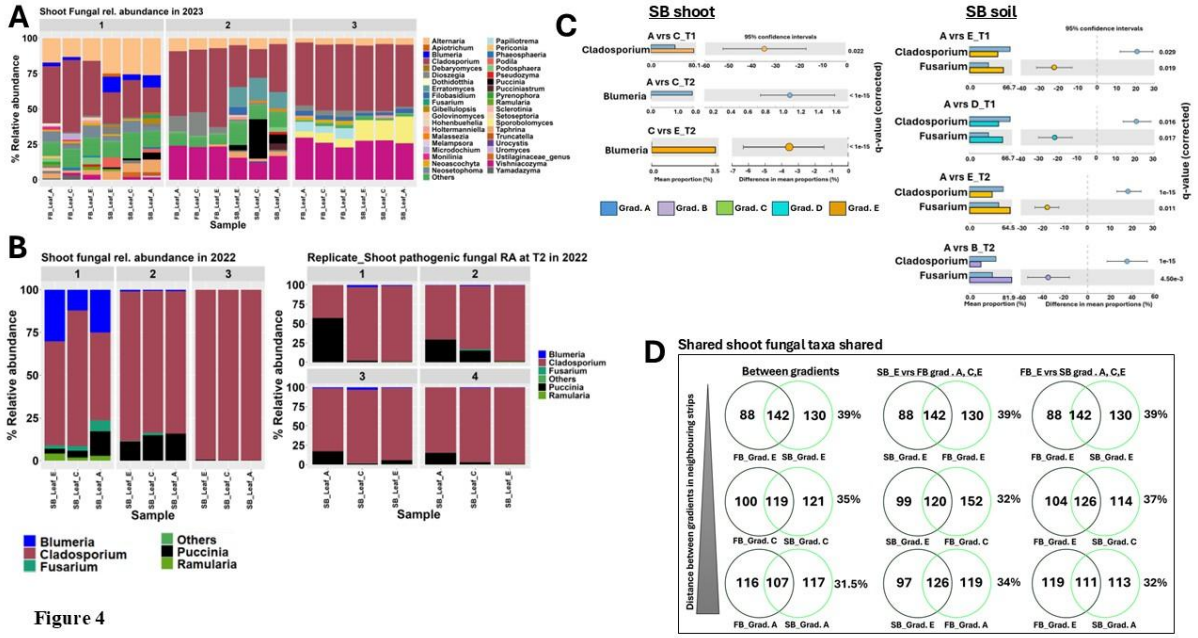

Figure 4

Figure 4. Shoot fungal communities within and across FB and SB strips in 2023. A) Bacterial relative abundances, B) relative abundances of potential shoot fungal pathogenic taxa in replicates of SB, C) relative abundances of potential shoot and soil fungal pathogenic taxa in SB and D) Number of shared shoot fungal taxa at different sampling locations within FB and SB in 2023.

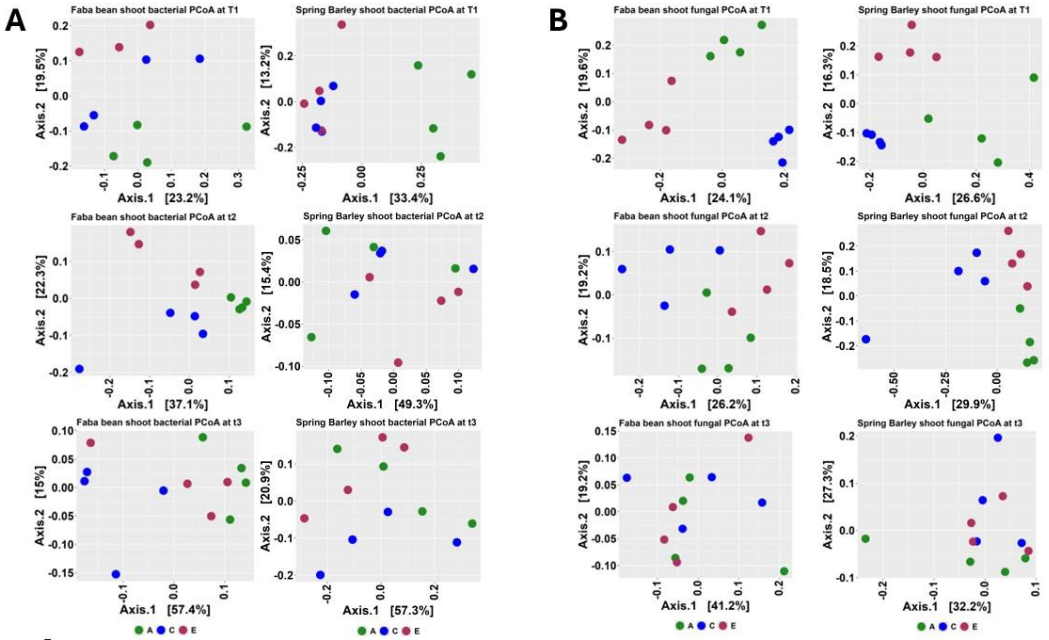

Figure 5.

Figure 5. PCoA of shoot microbial diversity within and across FB and SB strips in 2023. A) Bacterial community structures within and across FB and SB strips at different sampling times. B) Fungal community structures within and across FB and SB strips at different sampling times in 2023.

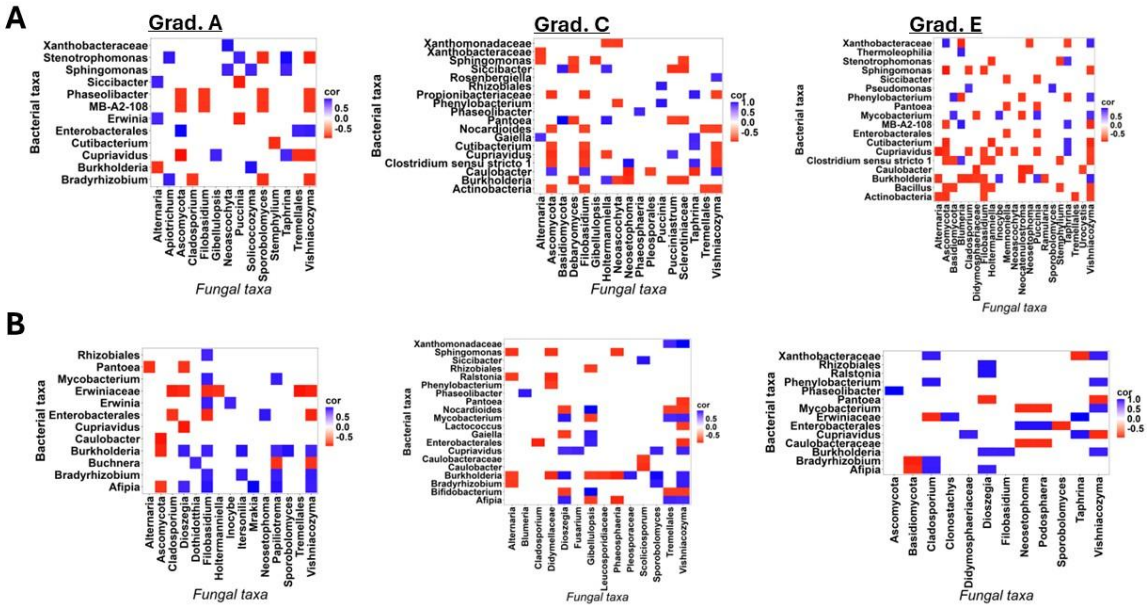

Figure 6.

Figure 6. Heat map showing significant correlations between bacterial and fungal taxa in A) SB and FB shoot samples. Bacterial and fungal data from all the time points were pooled and used for the analysis. We used ASVs present in at least 10 samples with Spearman's rank

correlations > 0.4 for positive correlations and <-0.4 for negative correlations, with $p < 0.05$, and correction using Benjamini-Hochberg fdr. Positive and negative correlations are indicated by blue and red colours, respectively.

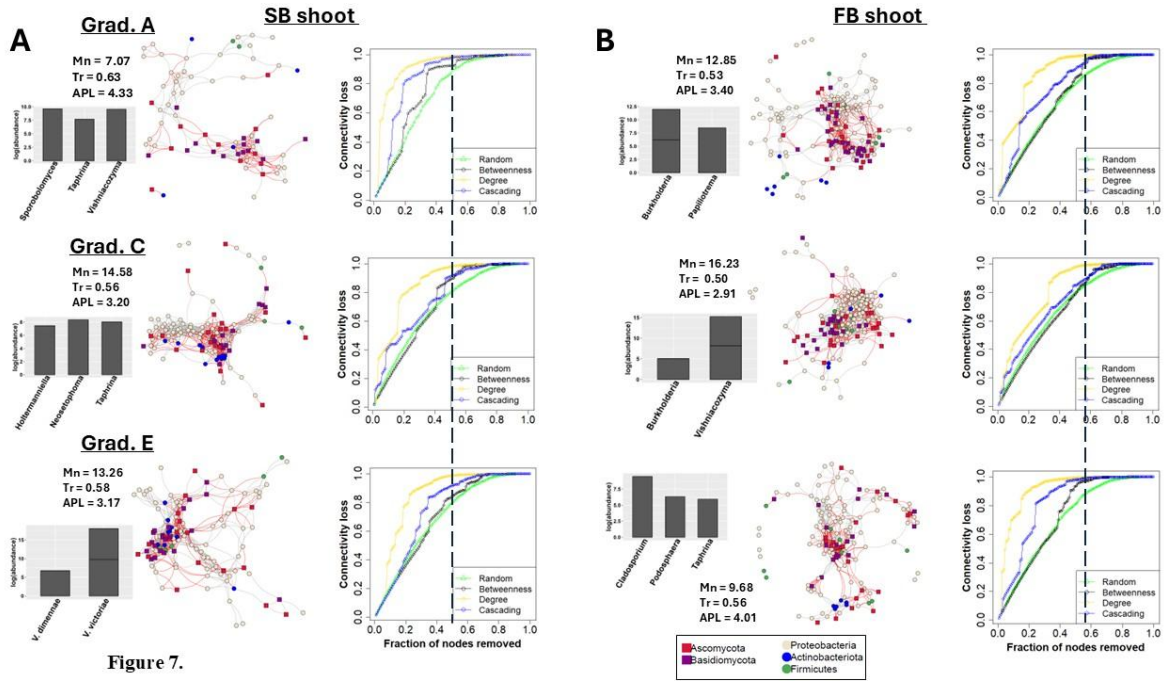

Figure 7.

Figure 7. Shoot microbial co-occurrence networks computed for the different sampling locations (centre to edge) in A) SB and B) FB. The grey and red edges represent positive and negative correlations, respectively. Network tolerance to attack of the respective site-specific networks using change in connectivity as a function of the fraction of removed nodes. Dashed lines show the maximum fraction of nodes to be removed for 100% connectivity loss (highest break-down of network) are shown. The four sustained attack strategies to test tolerance included random removal, direct removal of nodes with highest betweenness centrality, target on nodes with the highest impact closeness (degree), and a combination of random and targeted on betweenness (cascading). Additionally, relative abundance of hub taxa identified (including the numbers of ASVs assigned to phyla) for each site-specific network are shown.

Supplementary Figures

Figure S1: Differences in the abundances of potential fungal pathogenic genera in shoots between sampling locations A) A and E and B) C and E in FB, and C and E in SB at T2 in 2022. Analysis was performed with the STAMP software with White's nonparametric t test,

followed by Is Benjamini-Hochberg correction (FDR) with the parameters of q-value < 0.05. The ASVs are shown in the assigned taxon. The statistical test used was two-sided.

Figure S2: Soil bacterial relative abundance in faba bean (FB) and spring barley (SB) samples across strip gradients (from centre of strip towards the edge border rows (A-E)) at different sampling times in 2022.

Figure S3: Soil bacterial alpha diversity in faba bean (FB) and spring barley (SB) samples across strip gradients (from centre of strip towards the edge border rows (A-E)) at different sampling times in 2022.

Figure S4: A) Principal coordinate analysis (PCoA) plots of bacterial communites at different sampling sites in FB and SB strips at different time points in 2022. B) Indicator bacterial species characterizing different gradient positions in FB and SB spring fields in 2022.

Figure S5: Relative abundance of potential SB shoot fungal pathogenic genera in replicates at sampling times A) T2 and B) T3 in 2022.

Figure S6: Relative abundance of soil fungi at sampling time A) 1, 2 and B) sampling time 3 in 2022.

Figure S7: Relative abundance of potential soil fungal pathogens in SB sample replicates for the different sampling time points in 2022.

Figure S8: Differences in the abundances of potential fungal pathogenic genera in soil between gradient positions at T1 and T2 in SB. Analysis was performed with the STAMP software with White's nonparametric t test, followed by Benjamini-Hochberg correction (FDR) with the parameters of q-value < 0.05. The ASVs are shown in the assigned taxon. The statistical test used was two-sided.

Figure S9: Soil fungal alpha diversity in faba bean (FB) and spring barley (SB) samples across strip gradients (from centre of strip towards the edge border rows (A-E)) at different sampling times in 2022.

Figure S10: Principal coordinate analysis (PCoA) plots of soil fungal communities at different sampling sites in FB and SB strips at different time points in 2022.

Figure S11: Indicator soil fungal species characterizing different sampling locations in FB and SB spring fields using T1 and T2 datasets in 2022.

Figure S12: Indicator soil fungal species characterizing different sampling locations in FB and SB strips at T3 in 2022.

Figure S13: Shoot bacterial relative abundance in faba bean (FB) and spring barley (SB) samples across strip gradients (from centre of strip towards the edge border rows (A-E)) at different sampling times in 2023.

Figure S14: A) Soil bacterial and B) fungal relative abundances in faba bean (FB) and spring barley (SB) samples across strip gradients (from centre of strip towards the edge border rows (A-E)) at different sampling times in 2023.

Figure S15: Number of shared shoot bacterial taxa at different sampling locations within FB and SB in 2023.

Figure S16: Shoot and soil bacterial alpha diversity in faba bean (FB) and spring barley (SB) samples across strip gradients (from centre of strip towards the edge border rows (A-E)) at different sampling times in 2023.

Figure S17: Shoot and soil fungal alpha diversity in faba bean (FB) and spring barley (SB) samples across strip gradients (from centre of strip towards the edge border rows (A-E)) at different sampling times in 2023.

Figure S18: Principal coordinate analysis (PCoA) plots of soil microbial communities at different sampling sites in FB and SB strips at different time points in 2023.

Figure S19: Indicator soil microbial species characterizing different sampling locations in FB and SB spring fields in 2023.

Figure S20: Barplot of predicted functions at sampling location using shoot bacterial dataset in 2023. Significant differences ($P < 0.05$) between functions at sampling sites are indicated in letters after false-discovery rate (FDR) correction. Error bars denote the standard error (SE) of the mean relative abundance.

Figure S21: Barplot of predicted functions at sampling location using soil bacterial dataset in 2023. Significant differences ($P < 0.05$) between functions at sampling sites are indicated in

letters after false-discovery rate (FDR) correction. Error bars denote the standard error (SE) of the mean relative abundance.

Figure S22: Barplot of predicted functions at sampling location using shoot fungal dataset in 2023. Significant differences (P< 0.05) between functions at sampling sites are indicated in letters after false-discovery rate (FDR) correction. Error bars denote the standard error (SE) of the mean relative abundance.

Figure S23: Barplot of predicted functions at sampling location SB using soil fungal dataset in 2023. Significant differences (P< 0.05) between functions at sampling sites are indicated in letters after false-discovery rate (FDR) correction. Error bars denote the standard error (SE) of the mean relative abundance.

Figure S24: Barplot of predicted functions at sampling location using FB soil fungal dataset in 2023. Significant differences (P< 0.05) between functions at sampling sites are indicated in letters after false-discovery rate (FDR) correction. Error bars denote the standard error (SE) of the mean relative abundance.

Figure S25: Heat map showing significant correlations between bacterial and fungal taxa in A) SB and B) FB soil samples. Bacterial and fungal data from all the time points were pooled and used for the analysis. We used ASVs present in at least 10 samples with Spearman's rank correlations > 0.4 for positive correlations and <-0.4 for negative correlations, with $p < 0.05$, and correction using Benjamini-Hochberg FDR. Positive and negative correlations are indicated by blue and red colours, respectively.

Figure S26: Soil microbial co-occurrence networks computed for the different sampling locations (centre to edge sites) in A) SB and B) FB samples. The grey and red edges represent positive and negative correlations, respectively. Network tolerance to attack of the respective site-specific networks using change in connectivity as a function of the fraction of removed nodes. Dashed lines show the maximum fraction of nodes to be removed for 100% connectivity loss (highest break- down of network). The four sustained attack strategies to test tolerance included random removal, direct removal of nodes with highest betweenness centrality, target on nodes with the highest impact closeness (degree), and a combination of random and targeted on betweenness (cascading). Additionally, relative abundances of hub

taxa identified (including the numbers of ASVs assigned to phyla) for each site-specific networks are shown.

Supplementary Tables

Table S1: Faba bean (FB) and spring barley (SB) strip description including rotational seeding and fertilization.

Table S2: Sequence statistics including mean, median and range of reads per compartment for fungal and bacterial libraries at different days post inoculation (DPI) in 2022.

Table S3: Sequence statistics including mean, median and range of reads per compartment for fungal and bacterial libraries at different days post inoculation (DPI) in 2023.

Table S4: Shoot bacterial alpha diversity pair wise comparison (using Wilcoxon rank sum test) between strip gradient positions (from centre of strip towards the edge border rows (A-E)) of faba bean (FB) and spring barley (SB) samples at different sampling time T3 in 2022.

Table S5: Fungal shoot alpha diversity pair wise comparison (using Wilcoxon rank sum test) between strip gradient positions (from centre of strip towards the edge border rows (A-E)) of faba bean (FB) and spring barley (SB) samples at different sampling time T2 and T3 in 2022.

Table S6: Soil fungal alpha diversity pair wise comparison (using Wilcoxon rank sum test) between strip gradient positions (from centre of strip towards the edge border rows (A-E)) of faba bean (FB) and spring barley (SB) samples at different sampling time T2 and T3 in 2022.

Table S7: Summary of permutational analysis of variance (PERMANOVA) and Pairwise Adonis at each sampling time in 2022 using the “adonis” test on Bray-Curtis distance matrices using bacterial and fungal community dissimilarity assessment using 1,000 permutations.

Table S8: Shoot alpha diversity pair wise comparison (using Wilcoxon rank sum test) between strip gradient positions (from centre of strip towards the edge border rows (A-E)) of faba bean (FB) and spring barley (SB) samples at different sampling times in 2023.

Table S9: Soil alpha diversity pair wise comparison (using Wilcoxon rank sum test) between strip gradient positions (from centre of strip towards the edge border rows (A-E)) of faba bean (FB) and spring barley (SB) samples at different sampling times in 2023.

Table S10: Summary of permutational analysis of variance (PERMANOVA) and Pairwise Adonis at each sampling time in 2023 using the "adonis" test on Bray-Curtis distance matrices using bacterial and fungal community dissimilarity assessment using 1,000 permutations.

Table S11: Network metrics computed for gradient-specific networks of FB and SB using 2023 microbial datasets.

References

1. Li L, Tilman D, Lambers H, Zhang FS. Plant diversity and overyielding: Insights from belowground facilitation of intercropping in agriculture. New Phytol. 2014;203:63–9.

2. Alarcón-Segura V, Grass I, Breustedt G, Rohlfs M, Tscharntke T. Strip intercropping of wheat and oilseed rape enhances biodiversity and biological pest control in a conventionally managed farm scenario. J Appl Ecol. 2022;59:1513–23.

3. Liu J, Yang W. Soybean maize strip intercropping: A solution towards food security in China. J Integr Agric. 2024;23:2503–6.

4. Zhang Y, Bohan DA, Zhang C, Cong WF, Munier-Jolain N, Bedoussac L. Crop diversity reduces pesticide use more efficiently with refined diversification strategies. Commun Earth Environ. 2025;6:1–10.

5. Renard D, Tilman D. National food production stabilized by crop diversity. Nature 2019;571:257–60.

6. Beillouin D, Ben-Ari T, Malézieux E, Seufert V, Makowski D. Positive but variable effects of crop diversification on biodiversity and ecosystem services. Glob Chang Biol. 2021;27:4697–710.

7. Jiang P, Wang Y, Zhang Y, Fei J, Rong X, Peng J, et al. Intercropping enhances maize growth and nutrient uptake by driving the link between rhizosphere metabolites and microbiomes. New Phytol. 2024;243:1506–21.

8. Trinchera A, Migliore M, Warren Raffa D, Ommeslag S, Debode J, Shanmugam S, et al. Can multi-cropping affect soil microbial stoichiometry and functional diversity, decreasing

820 potential soil-borne pathogens? A study on European organic vegetable cropping systems.
821 Front Plant Sci. 2022;13.

822 9. Wang G, Bei S, Li J, Bao X, Zhang J, Schultz PA, et al. Soil microbial legacy drives crop
823 diversity advantage: Linking ecological plant–soil feedback with agricultural intercropping. J
824 Appl Ecol. 2021;58:496–506.

825 10. Trivedi P, Leach JE, Tringe SG, Sa T, Singh BK. Plant–microbiome interactions: from
826 community assembly to plant health. Nat Rev Microbiol. 2020;1–15.

827 11. Custódio V, Gonin M, Stabl G, Bakhoum N, Oliveira MM, Gutjahr C, et al. Sculpting the
828 soil microbiota. Plant J. 2022;109:508–22.

829 12. Kudjordjie EN, Hooshmand K, Sapkota R, Darbani B, Fomsgaard IS. Fusarium oxysporum
830 Disrupts Microbiome-Metabolome Networks in Arabidopsis thaliana Roots. Microbiol
831 Spectr. 2022;1–20.

832 13. Kudjordjie EN, Santos SS, Topalović O, Vestergård M. Distinct changes in tomato-
833 associated multi- kingdom microbiomes during Meloidogyne incognita parasitism. Environ
834 Microbiome. 2024;1–18.

835 14. Saleem M, Hu J, Jousset A. More Than the Sum of Its Parts: Microbiome Biodiversity as a
836 Driver of Plant Growth and Soil Health. Annu Rev Ecol Evol Syst. 2019;50:145–68.

837 15. Yang J, Ding D, Zhang X, Gu H. A comparative analysis of soil physicochemical properties
838 and microbial community structure among four shelterbelt species in the northeast China
839 plain. Microbiol Spectr. 2024;12:1–18.

840 16. Shi S, Richardson AE, O'Callaghan M, Deangelis KM, Jones EE, Stewart A, et al. Effects of
841 selected root exudate components on soil bacterial communities. FEMS Microbiol Ecol.
842 2011;77:600–10.

843 17. Bais HP, Weir TL, Perry LG, Gilroy S, Vivanco JM. the Role of Root Exudates in
844 Rhizosphere Interactions With Plants and Other Organisms. Annu Rev Plant Biol.
845 2006;57:233–66.

846 18. Broeckling CD, Broz AK, Bergelson J, Manter DK, Vivanco JM. Root exudates regulate soil
847 fungal community composition and diversity. Appl Environ Microbiol. 2008;74:738–44.

19. Lynch JM, Whipps JM. Substrate flow in the rhizosphere. Plant Soil. 1990;129:1–10.

20. Whipps JM, Hand P, Pink D, Bending GD. Phyllosphere microbiology with special reference to diversity and plant genotype. 2008;105:1744–55.

21. Vorholt J a. Microbial life in the phyllosphere. Nat Rev Microbiol. 2012;10:828–40.

22. Singh P, Santoni S, This P, Jean-pierre P. Genotype-environment interaction shapes the microbial assemblage in grapevine ' s phyllosphere and carposphere : An NGS approach. Microorganisms. 2018; 2018, *6*, 96.

23. Yan K, Han W, Zhu Q, Li C, Dong Z, Wang Y. Leaf surface microtopography shaping the bacterial community in the phyllosphere: evidence from 11 tree species. Microbiol Res [2022;254:126897.

24. Qian X, Duan T, Sun X, Zheng Y, Wang Y, Guo L, et al. Host genotype strongly in fl uences phyllosphere fungal communities associated with Mussaenda pubescens var . alba (Rubiaceae). Fungal Ecol 2018;36:141–51.

25. Bell-Dereske LP, Benucci GMN, da Costa PB, Bonito G, Friesen ML, Tiemann LK, et al. Regional biogeography versus intra-annual dynamics of the root and soil microbiome. Environ Microbiome. 2023;18:1–19.

26. Baltrus DA. Bacterial dispersal and biogeography as underappreciated influences on phytobiomes. Curr Opin Plant Biol. 2020;56:37–46.

27. Morella NM, Weng FCH, Joubert PM, Jessica C, Lindow S, Koskella B. Successive passaging of a plant-associated microbiome reveals robust habitat and host genotype-dependent selection. PNAS. 2020;117:1148–59.

28. Vos M, Wolf AB, Jennings SJ, Kowalchuk GA. Micro-scale determinants of bacterial diversity in soil. FEMS Microbiol Rev. 2013;37:936–54.

29. Hassani MA, Durán P, Hacquard S. Microbial interactions within the plant holobiont. Microbiome. Microbiome; 2018;6:58.

30. Mészárošová L, Kuťáková E, Kohout P, Münzbergová Z, Baldrian P. Plant effects on microbiome composition are constrained by environmental conditions in a successional grassland. Environ Microbiome. 2024;19:1–12.

876 31. Meyer KM, Porch R, Muscettola IE, Vasconcelos ALS, Sherman JK, Metcalf CJE, et al.
877 Plant neighborhood shapes diversity and reduces interspecific variation of the phyllosphere
878 microbiome. ISME J. Springer US; 2022;16:1376–87.

879 32. Huss CP, Holmes KD, Blubaugh CK. Benefits and Risks of Intercropping for Crop
880 Resilience and Pest Management. J Econ Entomol. 2022;115:1350–62.

881 33. Liao HL, Bonito G, Hameed K, Wu SH, Chen KH, Labbé J, et al. Heterospecific Neighbor
882 Plants Impact Root Microbiome Diversity and Molecular Function of Root Fungi. Front
883 Microbiol. 2021;12:1–15.

884 34. Zhao X, Dong Q, Han Y, Zhang K, Shi X, Yang X, et al. Maize/peanut intercropping
885 improves nutrient uptake of side-row maize and system microbial community diversity.
886 BMC Microbiol. 2022;22:1–16.

887 35. Ampt EA, van Ruijven J, Zwart MP, Raaijmakers JM, Termorshuizen AJ, Mommer L. Plant
888 neighbours can make or break the disease transmission chain of a fungal root pathogen.
889 New Phytol. 2022;233:1303–16.

890 36. Brennan EB. Agronomy of strip intercropping broccoli with alyssum for biological control
891 of aphids. Biol Control. 2016;97:109–19.

892 37. Li L, Sun J, Zhang F, Li X, Yang S, Rengel Z. Wheat/maize or wheat/soybean strip
893 intercropping I. Yield advantage and interspecific interactions on nutrients. F Crop Res.
894 2001;71:123–37.

895 38. Chelius MK, Triplett EW. The diversity of archaea and bacteria in association with the
896 roots of Zea mays L. Microb Ecol. 2001;41:252–63.

897 39. Beckers B, Op De Beeck M, Thijs S, Truyens S, Weyens N, Boerjan W, et al. Performance
898 of 16s rDNA primer pairs in the study of rhizosphere and endosphere bacterial microbiomes
899 in metabarcoding studies. Front Microbiol. 2016;7:650.

900 40. Bodenhausen N, Horton MW, Bergelson J. Bacterial Communities Associated with the
901 Leaves and the Roots of Arabidopsis thaliana. PLoS One. 2013;8.

902 41. Ihrmark K, Bödeker ITM, Cruz-Martinez K, Friberg H, Kubartova A, Schenck J, et al. New
903 primers to amplify the fungal ITS2 region--evaluation by 454-sequencing of artificial and

natural communities. FEMS Microbiol Ecol. The Oxford University Press; 2012;82:666–77.

42. White TJ, Bruns T, Lee S, Taylor J. Amplification and direct sequencing of fungal ribosomal RNA genes for phylogenetics. In: Innis MA, Gelfland DH, Sninsky JJ & White TJ eds. pp. 315–322, editor. PCR Protoc A Guid to Methods Appl. San Diego; 1990. p. 315–22.

43. Kudjordjie EN, Sapkota R, Steffensen SK, Fomsgaard IS, Nicolaisen M. Maize synthesized benzoxazinoids affect the host associated microbiome. Microbiome. 2019;1–17.

44. Kudjordjie EN, Desmedt W, Kyndt T. Diterpenoid Phytoalexins Shape Rice Root Microbiomes and Their Associations With Root Parasitic Nematodes. Environ Microbiol. 2025; 27:e70084.

45. Callahan BJ, McMurdie PJ, Rosen MJ, Han AW, Johnson AJA, Holmes SP. DADA2: High-resolution sample inference from Illumina amplicon data. Nat Methods. 2016;13:581–3.

46. Quast C, Pruesse E, Yilmaz P, Gerken J, Schweer T, Yarza P, et al. The SILVA ribosomal RNA gene database project: Improved data processing and web-based tools. Nucleic Acids Res. 2013;41:590–6.

47. Nilsson RH, Larsson KH, Taylor AFS, Bengtsson-Palme J, Jeppesen TS, Schigel D, et al. The UNITE database for molecular identification of fungi: Handling dark taxa and parallel taxonomic classifications. Nucleic Acids Res. 2019;47:D259–64.

48. R Core Team. R : A Language and Environment for Statistical Computing. 2022. https://www.r-project.org/

49. Oksanen AJ, Blanchet FG, Friendly M, Kindt R, Legendre P, Mcglinn D, et al. Package ' vegan .' 2020;3. https://cran.r-project.org/web/packages/vegan/index.html.

50. McMurdie PJ, Holmes S, Kindt R, Legendre P, O'Hara R. phyloseq: An R Package for Reproducible Interactive Analysis and Graphics of Microbiome Census Data. Watson M, editor. PLoS One. 2013;8:e61217.

51. Wickham H. ggplot2: Elegant Graphics for Data Analysis. Media. 2009. Available from: http://link.springer.com/10.1007/978-0-387-98141-3

52. Parks DH, Beiko RG. Identifying biologically relevant differences between metagenomic communities. Bioinformatics. 2010;26:715–21.

53. Parks DH, Tyson GW, Hugenholtz P, Beiko RG. STAMP: Statistical analysis of taxonomic and functional profiles. Bioinformatics. 2014;30:3123–4.

54. Benjamini Y, Hochberg Y. Controlling the false discovery rate: a practical and powerful approach to multiple testing. J R Stat Soc Ser B. 1994;57:289–300.

55. Liu C, Cui Y, Li X, Yao M. Microeco: An R package for data mining in microbial community ecology. FEMS Microbiol Ecol. Oxford University Press; 2021;97:1–9.

56. Dufrene M, Legendre P. Species assemblages and indicator species : the need for a flexible asymmetrical approach . Ecol. Monogr. 1997;345:1–17.

57. Roberts DW. Package 'labdsv': Ordination and Multivariate Analysis for Ecology. R Packag ver 16–1. 2013;1–56. https://cran.r-project.org/web/packages/labdsv/index.html.

58. Louca S, Polz MF, Mazel F, Albright MBN, Huber JA, O'Connor MI, et al. Function and functional redundancy in microbial communities. Nat Ecol Evol. 2018;2:936–43.

59. Põlme S, Abarenkov K, Henrik Nilsson R, Lindahl BD, Clemmensen KE, Kauserud H, et al. FungalTraits: a user-friendly traits database of fungi and fungus-like stramenopiles. Fungal Divers. 2020; 105, 1–16.

60. Robinson MD, McCarthy DJ, Smyth GK. edgeR: A Bioconductor package for differential expression analysis of digital gene expression data. Bioinformatics. 2010;26:139–40.

61. Csardi G, Nepusz T. The igraph software package for complex network research. InterJournal Complex Syst. 2006;Complex Sy:1695. Available from: http://igraph.sf.net

62. Xiao X, Han L, Chen H, Wang J, Zhang Y, Hu A. Intercropping enhances microbial community diversity and ecosystem functioning in maize fields. Front Microbiol. 2023;13:1–11.

63. Diaz-Troya S, Huertas MJ. Green microbes: Potential solutions for key sustainable development goals. Microb Biotechnol. 2024;17:1–8.

64. Stewart PS, Franklin MJ. Physiological heterogeneity in biofilms. Nat Rev Microbiol. 2008;6:199–210.

65. Bai Y, Müller DB, Srinivas G, Garrido-Oter R, Potthoff E, Rott M, et al. Functional overlap

959 of the Arabidopsis leaf and root microbiota. Nature. 2015;528:364–9.

960 66. Liu L, Gao Y, Gao Z, Zhu L, Yan R, Yang W, et al. The core microbiota as a predictor of soil
961 functional traits promotes soil nutrient cycling and wheat production in dryland farming.
962 Funct Ecol. 2023;37:2325–37.

963 67. Giongo A, Arnhold J, Grunwald D, Smalla K, Braun-Kiewnick A. Soil depths and
964 microhabitats shape soil and root-associated bacterial and archaeal communities more than
965 crop rotation in wheat. Front Microbiomes. 2024;3:1–14.

966 68. Almario J, Mahmoudi M, Kroll S, Agler M, Placzek A, Mari A, et al. The Leaf Microbiome
967 of Arabidopsis Displays Reproducible Dynamics and Patterns throughout the Growing
968 Season. MBio. American Society for Microbiology; 2022;13.

969 69. Edwards JA, Santos-Medellín CM, Liechty ZS, Nguyen B, Lurie E, Eason S, et al.
970 Compositional shifts in root-associated bacterial and archaeal microbiota track the plant life
971 cycle in field-grown rice. PLoS Biol. 2018;16:1–28.

972 70. Micallef S, Colón-Carmona A. Genetic and Developmental Control of Rhizosphere
973 Bacterial Communities. Mol Microb Ecol Rhizosph. 2013;1:257–63.

974 71. Quiza L, Tremblay J, Pagé AP, Greer CW, Pozniak CJ, Li R, et al. The effect of wheat
975 genotype on the microbiome is more evident in roots and varies through time. ISME
976 Commun. 2023;3:1–10.

977 72. Labouyrie M, Ballabio C, Romero F, Panagos P, Jones A, Schmid MW, et al. Patterns in
978 soil microbial diversity across Europe. Nat Commun. 2023;14.

979 73. Liu M, Zhou T, Fu Q. Leaf nitrogen and phosphorus are more sensitive to environmental
980 factors in dicots than in monocots, globally. Plant Divers. 2024;46:804–11.

981 74. Sangiorgio D, Cáliz J, Mattana S, Barceló A, De Cinti B, Elustondo D, et al. Host species
982 and temperature drive beech and Scots pine phyllosphere microbiota across European
983 forests. Commun Earth Environ. 2024;5:1–10.

984 75. Brandl MT, Mammel MK, Simko I, Richter TKS, Gebru ST, Leonard SR. Weather factors,
985 soil microbiome, and bacteria-fungi interactions as drivers of the epiphytic phyllosphere
986 communities of romaine lettuce. Food Microbiol. 2023;113:104260.

76. Singh RP, Hodson DP, Huerta-Espino J, Jin Y, Bhavani S, Njau P, et al. The emergence of Ug99 races of the stem rust fungus is a threat to world wheat production. Annu Rev Phytopathol. 2011;49:465–81.

77. Dentika P, Ozier-Lafontaine H, Penet L. Dynamics of Pathogenic Fungi in Field Hedges: Vegetation Cover Is Differentially Impacted by Weather. Microorganisms. 2022;10.

78. Pélissier R, Buendia L, Brousse A, Temple C, Ballini E, Fort F, et al. Plant neighbour-modulated susceptibility to pathogens in intraspecific mixtures. J Exp Bot. 2021;72:6570–80.

79. Zhou X, Zhang J, Shi J, Khashi U Rahman M, Liu H, Wei Z, et al. Volatile-mediated interspecific plant interaction promotes root colonization by beneficial bacteria via induced shifts in root exudation. Microbiome. 2024;12:207.

80. Tian B, Xie J, Fu Y, Cheng J, Li B, Chen T, et al. A cosmopolitan fungal pathogen of dicots adopts an endophytic lifestyle on cereal crops and protects them from major fungal diseases. ISME J. 2020;14:3120–35.

81. Finkel OM, Castrillo G, Herrera Paredes S, Salas González I, Dangl JL. Understanding and exploiting plant beneficial microbes. Curr. Opin. Plant Biol. 2017.

82. Duchateau S, Crouzet J, Dorey S, Aziz A. The plant-associated Pantoea spp. as biocontrol agents: Mechanisms and diversity of bacteria-produced metabolites as a prospective tool for plant protection. Biol Control. 2024;188.

83. Liu F, Hewezi T, Lebeis SL, Pantalone V, Grewal PS, Staton ME. Soil indigenous microbiome and plant genotypes cooperatively modify soybean rhizosphere microbiome assembly. BMC Microbiol. BMC Microbiology; 2019;19:1–19.

84. Liang D, Leung RKK, Guan W, Au WW. Involvement of gut microbiome in human health and disease: Brief overview, knowledge gaps and research opportunities. Gut Pathog. 2018;10:1–9.

85. Kempf HJ, Wolf G. *Erwinia herbicola* as a biocontrol agent of *Fusarium culmorum* and *Puccinia recondita* f. sp. *tritici* on wheat. Phytopathology. 1989. p. 990–4.

86. Krępski T, Piasecka A, Święcicka M, Kańczurzewska M, Sawikowska A, Dmochowska-Boguta M, et al. Leaf rust (Puccinia recondita f. sp. secalis) triggers substantial changes in rye

(Secale cereale L.) at the transcriptome and metabolome levels. BMC Plant Biol. 2024;24:1–26.

87. Kumar P, Kumar S, Jhilta P, Poria V, Yadav R, Singh S. Phosphate- and potassium-solubilizing Siccibacter colletis promotes wheat growth, yield, and nutrient uptake. J Appl Biol Biotechnol. 2024;13:51–61.

88. Wagg C, Schlaeppi K, Banerjee S, Kuramae EE, van der Heijden MGA. Fungal-bacterial diversity and microbiome complexity predict ecosystem functioning. Nat Commun. 2019;10:1–10.

89. Gao M, Xiong C, Gao C, Tsui CKM, Wang MM, Zhou X, et al. Disease-induced changes in plant microbiome assembly and functional adaptation. Microbiome. 2021;9:1–18.

90. Lurgi M, Galiana N, LÃ³pez BC, Joppa LN, Montoya JM. Network complexity and species traits mediate the effects of biological invasions on dynamic food webs. Front Ecol Evol. 2014;2:1–11.

91. Trivedi P, Delgado-Baquerizo M, Trivedi C, Hamonts K, Anderson IC, Singh BK. Keystone microbial taxa regulate the invasion of a fungal pathogen in agro-ecosystems. Soil Biol Biochem. 2017;111:10–4.

92. Fenta L, Mekonnen H, Gashaw T. Biocontrol potential of trichoderma and yeast against post harvest fruit fungal diseases: A review. WNOFNS. 27 (2019) 153-173

93. Bashi E, Fokkema NJ. Environmental factors limiting growth of Sporobolomyces roseus, an antagonist of Cochliobolus sativus, on wheat leaves. Trans Br Mycol Soc. 1977;68:17–25.

94. Zhong S, Ali S, Leng Y, Wang R, Garvin DF. Brachypodium distachyon-cochliobolus sativus pathosystem is a new model for studying plant-fungal interactions in cereal crops. Phytopathology. 2015;105:482–9.

95. Nian L, Xie Y, Zhang H, Wang M, Yuan B, Cheng S, et al. Vishniacozyma victoriae: An endophytic antagonist yeast of kiwifruit with biocontrol effect to Botrytis cinerea. Food Chem. 2023;411:135442.

96. Gorordo MF, Lucca ME, Sangorrín MP. Biocontrol Efficacy of the Vishniacozyma Victoriae in Semi-Commercial Assays for the Control of Postharvest Fungal Diseases of Organic Pears.

Curr Microbiol. 2022;79:1–7.

97. Liu S, Xie J, Luan W, Liu C, Chen X, Chen D. Papiliotrema flavescens, a plant growth-promoting fungus, alters root system architecture and induces systemic resistance through its volatile organic compounds in Arabidopsis. Plant Physiol Biochem. 2024;208:108474.

98. Compant S, Nowak J, Coenye T, Clément C, Ait Barka E. Diversity and occurrence of Burkholderia spp. in the natural environment. FEMS Microbiol Rev. 2008;32:607–26.

99. Kajihara KT, Hynson NA. Networks as tools for defining emergent properties of microbiomes and their stability. Microbiome. 2024;12:184.